

СООБЩЕНИЯ
ОБЪЕДИНЕННОГО
ИНСТИТУТА
ЯДЕРНЫХ
ИССЛЕДОВАНИЙ

Дубна

E4 - 6265



M.I.Baznat , M.I.Chernej , N.I.Pyatov

ЛАБОРАТОРИЯ ТЕОРЕТИЧЕСКОЙ ФИЗИКИ

**POLARIZATION EFFECTS
IN THE ROTATIONAL MOTION
OF ODD-MASS NUCLEI
III. Electromagnetic Properties
of Rotational States**

1972

E4 - 6265

M.I.Baznat*, M.I.Chernej*, N.I.Pyatov

POLARIZATION EFFECTS
IN THE ROTATIONAL MOTION
OF ODD-MASS NUCLEI

III. Electromagnetic Properties
of Rotational States

Научно-техническая
библиотека
ОИЯИ

* Institute of Applied Physics, AN MSSR (Kishinev)

Базнат М.И., Черней М.И., Пятов Н.И.

E4-6265

Поляризационные эффекты во вращательном движении нечетных атомных ядер. III . Электромагнитные свойства вращательных состояний

Исследованы электромагнитные свойства вращательных состояний в нечетных атомных ядрах, используя неадиабатическую вращательную модель. Развита процедура перенормировки колективных параметров J , g_R^0 и Q_0 четно-четного остова. Получено общее выражение для перенормировки спинового гиромагнитного отношения g_s с учетом взаимодействия Кориолиса. Проведен анализ экспериментальных данных в ряде атомных ядер.

Сообщение Объединенного института ядерных исследований
Дубна, 1972

Baznat M.I., Chernej M.I., Pyatov N.I. E4-6265

Polarization Effects in the Rotational Motion
of Odd-Mass Nuclei
III. Electromagnetic Properties of Rotational
States

Electromagnetic properties of rotational states in odd-mass nuclei are investigated employing the nonadiabatic rotational model developed in the preceding parts of this series. The equations for the renormalization of collective parameters J , g_R^0 and Q_0 of the even-even core in odd-mass nuclei are given. The general equation for the effective spin gyromagnetic factor g_s^{eff} including the effects of the spin polarization and Coriolis coupling is obtained. The analysis of experimental data in a number of rare-earth nuclei is carried out.

Communications of the Joint Institute for Nuclear Research.
Dubna, 1972

Introduction

The present paper is a continuation of the discussion of rotational states of odd-mass nuclei in the framework of the nonadiabatic model /1,2/. In the preceding parts of this series the method for the description of polarization effects induced by the residual interactions has been formulated and the analysis of strongly perturbed rotational bands in odd-N rare-earth nuclei has been carried out.

Nonadiabatic treatment of the rotation of odd-mass nuclei is based on the collective parameters of the even-even core (moment of inertia J , collective gyromagnetic ratio g_R^0 and intrinsic quadrupole moment Q_0). The corresponding effective quantities in odd-mass nuclei can be calculated in the model taking into account the coupling of an odd particle to the rotation and vibrations of the core. Among vibrational modes the I^+ states play an important role. The coupling of an odd particle to the I^+ states results in the well-known spin polarization effects /3/ (renormalization of g_s factor in magnetic moments). The spin-dependent and centrifugal interactions of an odd particle with the particles of the core lead to the renormalization of the Coriolis force. A satisfactory description of strongly perturbed rotational bands cannot be achieved without the account of polarization effects.

The rotational states are described by the wave function /1/

$$|IM\rangle = \sum_K C'_K |IMK\rangle , \quad (1)$$

where C'_K are K -mixing amplitudes of intrinsic states and $|IMK\rangle$ the normalized and symmetrized adiabatic wave functions. The energies of the corresponding states are given by the equation

$$\mathcal{E}(I) = \sum_K (C'_K)^2 \mathcal{E}_K + \frac{1}{2J} g(I) , \quad (2)$$

where \mathcal{E}_K are the energies of intrinsic states and the spectral function $g(I)$ is defined as

$$g(I) = I(I+1) - \sum_K (C_K^I)^2 K^2 + (-)^{I+1/2} (I+1/2) a(I) \quad (3)$$

The generalized decoupling parameter $a(I)$ is expressed through the diagonal matrix element of the Coriolis force operator H_C

$$a(I) = (-)^{I+1/2} (I+1/2)^{-1} 2J \langle IM | H_C | IM \rangle .$$

The effective moment of inertia of an odd-mass nucleus can be defined as follows

$$\frac{1}{2J_{\text{eff}}} [1 - \delta_{K,1/2} (-)^{I+1/2} a_{sp}] = \frac{\mathcal{E}(I+1) - \mathcal{E}(I)}{2(I+1)}, \quad (4)$$

where a_{sp} is the single-particle decoupling parameter. Inserting (2) in eq. (4) one obtains

$$\frac{\mathcal{E}(I+1) - \mathcal{E}(I)}{2(I+1)} = \frac{1}{2(I+1)} \sum_K \mathcal{E}_K [(C_K^{I+1})^2 - (C_K^I)^2] + \frac{1}{2(I+1)} \frac{1}{2J} [g(I+1) - g(I)]. \quad (5)$$

The first term of the right-hand side of eq. (5) represents the contribution to the effective moment of inertia from the rearrangement of the intrinsic spectra. The second term comes from the rotational energy. The former plays an important role in strongly perturbed rotational bands as will be shown below.

In the subsequent sections we discuss the electromagnetic properties of rotational states.

Magnetic Moments of Rotational States

In the Bohr's rotational model the magnetic dipole operator for an odd-mass nucleus is written in the form

$$\vec{\mu} = g_R^0 \vec{R} + g_s \vec{s} + g_\ell \vec{\ell}, \quad (6)$$

where \vec{R} is the collective rotational angular momentum and \vec{s} and $\vec{\ell}$ the spin and orbital particle momenta, respectively. The magnetic moment of the nucleus in the state $|IM\rangle$ is defined by

$$\mu_I = \frac{\langle IM | \vec{\mu} | IM \rangle}{I+1}. \quad (7)$$

Using the formalism of ref. 1/ we obtain

$$\mu_I = \frac{1}{I+1} \{ (g_R^0 - g_\ell) G(I) + g_\ell I(I+1) + (g_s - g_\ell) \langle IM | \vec{s} \vec{\ell} | IM \rangle \}, \quad (8)$$

where

$$G(I) = I(I+1) - \sum_K (C_K^I)^2 K^2 + 1/2 (-)^{I+1/2} (I+1/2) a(I). \quad (9)$$

The matrix element $\langle IM | \vec{s} \vec{\ell} | IM \rangle$ reads

$$\begin{aligned} \langle IM | \vec{s} \vec{\ell} | IM \rangle &= \sum_{K,K'} C_K^I C_{K'}^I (u_K u_{K'} + v_K v_{K'}) \{ \delta_{KK'} K \langle K | s_z | K \rangle R_\sigma(K, K') + \\ &+ \frac{1}{4} \sum_{r=\pm} r [s_{KK'}^{(r)} R_\sigma^{(r)}(K, K') \times \end{aligned}$$

$$\begin{aligned} & \times (\delta_{K',K+1} \sqrt{(I-K)(I+K+1)} + \delta_{K',K-1} \times \\ & \times \tau \sqrt{(I+K)(I-K+1)}) + \delta_{K,1/2} \delta_{K',1/2} \times \\ & \times (-)^{I+\ell+1/2} (I+1/2) s_{KK'}^{(\tau)} R_\sigma^{(i)}(K, K')] \} . \end{aligned} \quad (10)$$

It includes the effects of the Coriolis coupling as well as polarization effects from the spin-dependent and centrifugal residual forces. The single-particle matrix element $\langle K | s_z | K' \rangle$ is renormalized by the spin-dependent force alone and the corresponding renormalization factor R_σ (longitudinal spin polarization) was calculated in ref. /3/. The matrix element $s_{KK'}^{(\tau)}$ (for the definitions see ref. /1/) is renormalized by both the spin-dependent and centrifugal forces. The renormalization factor $R_\sigma^{(i)}$ (transverse polarization) reads

$$\begin{aligned} R_\sigma^{(i)}(K, K') = N_K N_{K'} \{ 1 - & \frac{\kappa s_{KK'}^{(i)}}{1 + \kappa s_{KK'}^{(i)}} - \\ - & \frac{\kappa s_{K'K}^{(i)}}{1 + \kappa s_{K'K}^{(i)}} - \frac{i_{KK'}^{(\tau)}}{\sigma_{KK'}^{(\tau)}} [\frac{1}{1 + \kappa s_{KK'}^{(i)}} \times \\ & \times \frac{X_{KK'}}{2J + J_{KK'}} + \frac{1}{1 + \kappa s_{K'K}^{(i)}} \frac{X_{K'K}}{2J + J_{K'K}}] \} . \end{aligned} \quad (II)$$

In adiabatic approximation eq. (8) takes the well-known form (see, e.g., ref. /4/)

$$\begin{aligned} \mu_I = \frac{1}{I+1} \{ (g_R^{\text{eff}} - g_\ell) G_K(I) + g_\ell I(I+1) + \\ + (g_s^{\text{eff}} - g_\ell) \langle IMK | \vec{s} \vec{l}^\dagger | IMK \rangle \} , \end{aligned} \quad (12)$$

where

$$G_K(I) = I(I+1) - K^2 + 1/2 \delta_{K,1/2} (-)^{I+1/2} (I+1/2) a_{sp} \quad (13)$$

$$\begin{aligned} \langle IMK | \vec{s} \vec{l}^\dagger | IMK \rangle = K \langle K | s_z | K \rangle + \\ + 1/2 \delta_{K,1/2} (-)^{I+1/2} (I+1/2) \langle K | s_+ | -K \rangle . \end{aligned} \quad (14)$$

One can see that both the polarization and Coriolis coupling effects in magnetic moments can be reduced to the renormalization of the parameters g_R^0 and g_s . The quantity g_R^{eff} , in our approach, depends on the spin value and can be calculated from the equation ^{x/}:

$$g_R^{\text{eff}} - g_\ell = (g_R^0 - g_\ell) \frac{G(I)}{G_K(I)} . \quad (15)$$

From eq. (15) it follows an obvious difference of g_R^{eff} values for the odd-N and odd-Z nuclei (see Fig. 1a). For the states of the lowest-energy rotational band of a given parity the following estimate $|G(I)/G_K(I)| \leq 1$ usually holds that leads to

$$g_R^{\text{eff}}(N) \leq g_R^0 \leq g_R^{\text{eff}}(Z) . \quad (16)$$

^{x/} We assume here that the quantity g_ℓ is not renormalized by the forces included in the model.

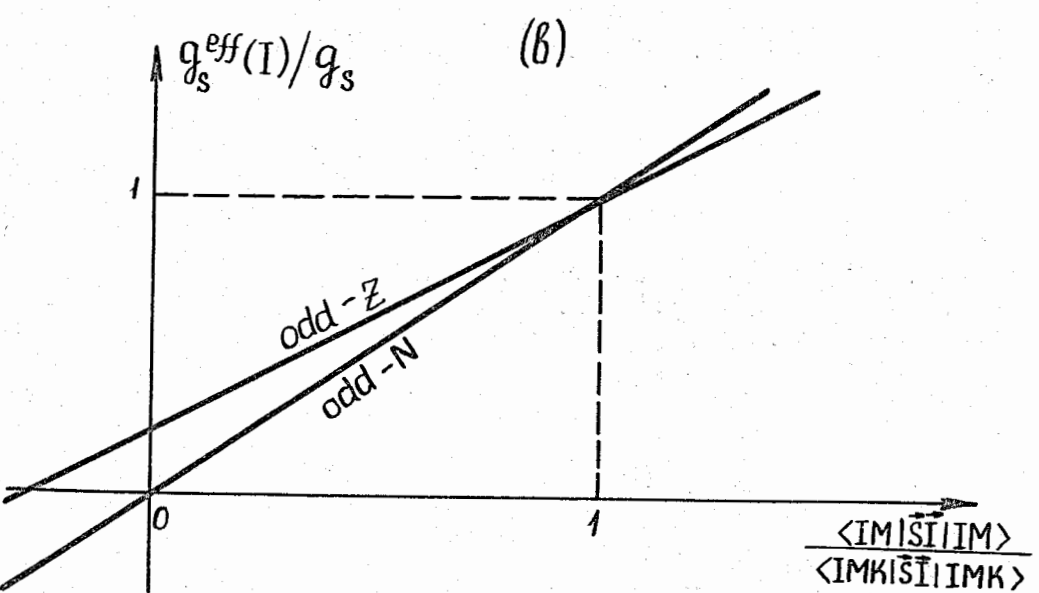
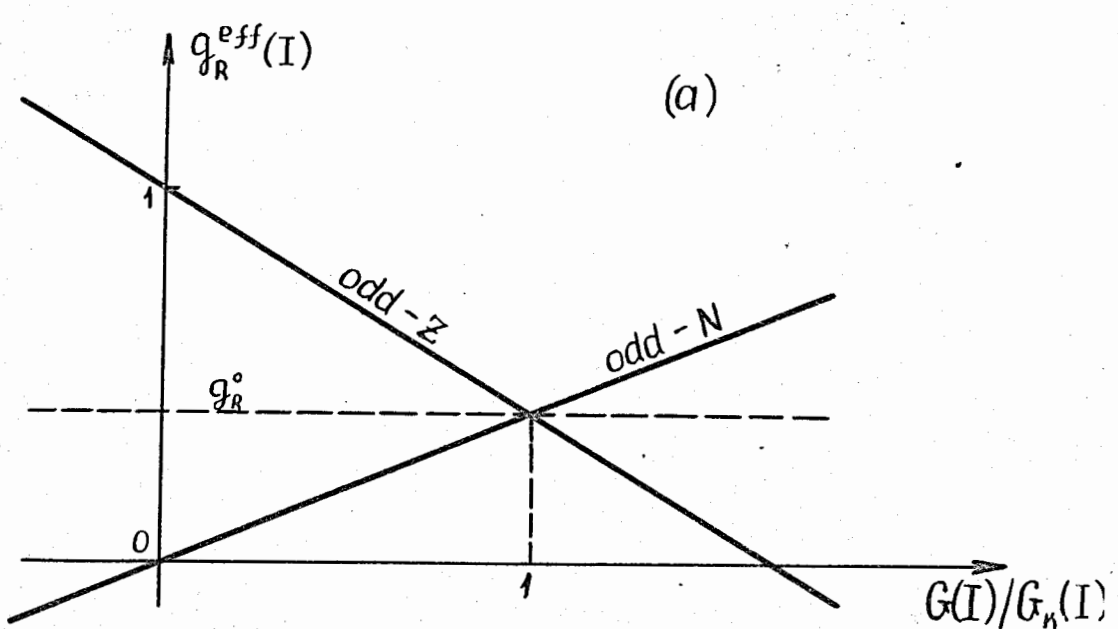


Fig. I. Renormalization of g_R^0 (a) and g_s (b) factors in odd-N and odd-Z nuclei.

These inequalities agree qualitatively with experimental data (see, e.g., ref./5/) and theoretical estimates /6/ in the cranking model. It is easy to obtain the approximate equation for g_R^{eff} for high spin states

$$(g_R^{eff} - g_\ell)_{I \gg 1} \approx (g_R^0 - g_\ell) [1 - \frac{|\alpha(I)|}{2I}] . \quad (17)$$

One can see that g_R^{eff} tends to g_R^0 with increasing spin value because the quantity $|\alpha(I)|$ tends to be saturated for high-spin states.

The renormalization of the g_s factor can be defined by the following equation

$$g_s^{eff} - g_\ell = (g_s - g_\ell) \frac{\langle IM | \vec{s} \vec{l}' | IM \rangle}{\langle IMK | \vec{s} \vec{l}' | IMK \rangle} . \quad (18)$$

Both the polarization and Coriolis force effects are included into eq. (18). Due to the Coriolis coupling, the effects of the longitudinal and transverse polarizations cannot be separated. In adiabatic approximation the renormalization of g_s is determined by the longitudinal R_a and transverse R_d^{eff} polarization factors. The difference of g_s^{eff} for the odd-N and odd-Z nuclei is demonstrated in Fig. 1b.

Note that the function $G(I)$ is closely related to the spectral function $\alpha(I)$. Hence the expected values of μ_I can be calculated in the model after fitting the energy spectra (g_R^0 is known from neighbouring even-even nuclei).

MI and E2 Transitions within Rotational Band

The MI transition operator is written in the laboratory frame of reference

$$\overline{M} (M1, \nu) = \sqrt{\frac{3}{4\pi}} \mu_N D_\nu \quad (19)$$

with definitions

$$D_0 = (g_s - g_\ell) s_z + (g_\ell - g_R^0) i_z ,$$

$$D_{\pm} = \mp \frac{1}{\sqrt{2}} [(g_s - g_\ell) s_{\pm} + (g_\ell - g_R^0) i_{\pm}]$$

$(\mu_N \equiv e\hbar / 2Mc).$

Using the wave functions (I) one obtains the following expression for the reduced transition probability

$$\begin{aligned} B(M1, I' \rightarrow I) &= \frac{3}{4\pi} \mu_N^2 \left| \sum_{K,K'} C_K^{I'} C_{K'}^{I'} \times \right. \\ &\times (u_K u_{K'} + v_K v_{K'}) \{ \delta_{KK'} \langle I' 1 K 0 | IK \rangle \times \\ &\times [(g_s - g_\ell) \langle K | s_z | K \rangle R_\sigma + K (g_\ell - g_R^0)] + \\ &+ \frac{1}{2\sqrt{2}} \sum_{r=\pm} [(g_s - g_\ell) s_{KK'}^{(r)} R_\sigma^{(r)} (K, K') + \\ &+ (g_\ell - g_R^0) i_{KK'}^{(r)} R_i^{(r)} (K, K')] [\tau \delta_{K', K+1} \times \\ &\times \langle I' 1 K+1 - 1 | IK \rangle - \delta_{K', K-1} \langle I' 1 K-1 | IK \rangle] \} |^2 . \end{aligned} \quad (20)$$

$$\begin{aligned} &+ \delta_{K,1/2} \delta_{K',1/2} (-)^{l+l+1/2} \langle I' 1 \frac{1}{2} - 1 | I - \frac{1}{2} \rangle \times \\ &\times \frac{1}{2\sqrt{2}} \sum_{r=\pm} r [(g_s - g_\ell) s_{KK'}^{(r)} R_\sigma^{(r)} (K, K') + \end{aligned}$$

$$+ (g_\ell - g_R^0) i_{KK'}^{(r)} R_i^{(r)} (K, K')] \} |^2 ,$$

where the single-particle matrix elements $s_{KK'}^{(r)}$, $i_{KK'}^{(r)}$, and polarization factors $R_i^{(r)}(K, K')$ are defined as in ref. [1]. It is clear that in eq. (20) the nonadiabatic effects cannot be reduced to the renormalization of g_R^0 and g_s factors which is determined by eqs. (15) and (18), e.i., the effective parameters g_K and g_R^{eff} calculated from observed $B(M1)$ values in adiabatic approximation will differ from those extracted from magnetic moments.

The Coriolis force perturbs the electric properties of rotational states much weaker than the magnetic ones. For the spectroscopic quadrupole moment of the nucleus in the state $|IM=I\rangle$ one obtains

$$Q_I \approx Q_0 \frac{3 \sum_K (C_K^{I'})^2 K^2 - I(I+1)}{(I+1)(2I+3)} \quad (21)$$

where Q_0 is the intrinsic quadrupole moment whose magnitude is close to that of the even-even core (there may be some difference because of the contribution of the odd particle as well as due to the coupling of rotation to quadrupole vibrations of the core). The intraband reduced E2-transition probability may be obtained in the same approximation as eq. (21).

$$B(E2, I' \rightarrow I) \approx \frac{5}{16\pi} e^2 Q_0^2 \left| \sum_K C_K^{I'} C_{K'}^{I'} \langle I' 2 K 0 | IK \rangle \right|^2 . \quad (22)$$

It was shown in ref. [1] that the branching ratio $B(E2, I \rightarrow I-2) / B(E2, I \rightarrow I-1)$ deviates noticeably from the Alaga rule only in rotational bands strongly distorted by the Coriolis force. Nonadiabatic effects in eqs. (21) and (22) may be reduced to the renormalization of the Q_0 value. But in general the effective values of Q_0^{eff} , obtained from spectroscopic quadrupole moments and those extracted from the $B(E2)$ values may be different. Moreover, in the case of strong Coriolis coupling the effective Q_0^{eff} quantities derived from $B(E2, I \rightarrow I+1)$ and $B(E2, I \rightarrow I-2)$ are different as well.

The intraband mixing ratio δ_I^2 and the crossover-to-cascade intensity ratio λ_I defined by the usual equations

$$\delta_I^2 \equiv \frac{T_\gamma(E2, I \rightarrow I-1)}{T_\gamma(M1, I \rightarrow I-1)}, \quad (23)$$

$$\lambda_I \equiv \frac{T_\gamma(E2, I \rightarrow I-2)}{T_\gamma(E2, I \rightarrow I-1)} - \frac{\delta_I^2}{1 + \delta_I^2} \quad (24)$$

are much more sensitive to the non-adiabatic effects. In eqs. (23) and (24) T_γ is the γ -transition probability.

The effective adiabatic parameter $[(g_K - g_R)/Q_0]^2_{eff}$ can be calculated from the following equation

$$[\frac{g_K - g_R}{Q_0}]^2_{eff} \equiv \frac{1}{\delta_I^2} \frac{E_\gamma(\text{MeV})}{0.287(2I+1)(2I-2)}. \quad (25)$$

In the general case this parameter is not constant in the rotational band.

Details of Calculation and Discussion

For the description of the nuclear average field we use the deformed Saxon-Woods potential. The method of solution of the Schrödinger equation with such a potential has been derived in ref. /7/. The numerical parameters of the Saxon-Woods potential used in our calculations are given in ref. /8/. The deformation parameter β_{20} was chosen to be 0.32 for the Gd, Dy and Er isotopes and 0.24 for Hf isotopes (β_{40} was put to be zero). As a rule the calculated energies are not very sensitive to this parameter /2/. But sometimes the electromagnetic properties of rotational states strongly depend on the deformation, as will be shown below for ^{155}Gd .

For each nucleus the static equations for the energy gap Δ and chemical potential λ were solved (without blocking which is weakened by the Coriolis coupling). Then the quasiparticle spectra and polarization factors R_σ , $R_\sigma^{(i)}$ and $R_i^{(\sigma)}$ were calculated (with-

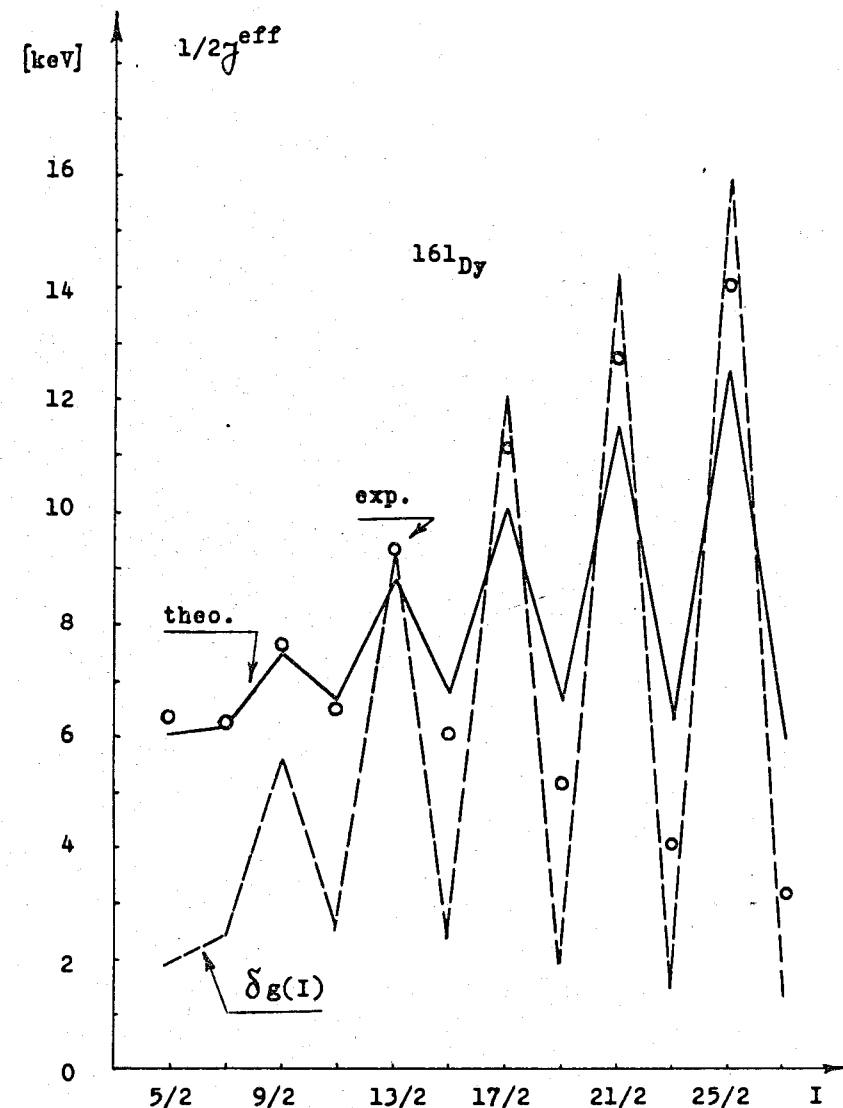


Fig. 2. Calculated effective inverse moment of inertia $1/2J_{eff}$ (solid line) and the quantity $\delta_g(I)$ (eq. (26)) (dashed line) versus spin value in the ground band of ^{161}Dy . Experimental values /2/ are given by open circles.

out blocking, too). The Coriolis force matrix was diagonalized in a restricted space of quasiparticle states (usually about 7-10 states of the same parity, connected by the large matrix element $i_{KK}^{(r)}$; some extent of the space leads to a small renormalization of the rotational parameter $1/2J$).

It has been noted in ref. /2/ that in the case of strong Coriolis coupling the spacing among low-energy states of rotational band depends much stronger on the intrinsic spectra (or the Δ value in our model) than on the value of the rotational parameter $1/2J$. Indeed, the rearrangement of the intrinsic spectra brings an essential contribution to the effective inverse moment of inertia $1/2J^{\text{eff}}$ (see eqs. (4) and (5)), as is demonstrated in Fig. 2 for ^{161}Dy . The contribution of the rotational energy

$$\delta g(I) = \frac{1}{2(I+1)} - \frac{1}{2J} [g(I+1) - g(I)] \quad (26)$$

does not exceed 30-40% of the total $1/2J^{\text{eff}}$ in many states of the rotational band, that explains the relatively weak dependence of the rotational spectra on the value of $1/2J$.

The isospin-dependent strength parameter κ of the spin-spin residual force /1/ has been determined from calculations of magnetic moments and comparison with experimental data. The dependence of μ_I on parameters κ and g_R^0 is shown in Fig. 3 for the ground state of ^{161}Dy . Systematic calculations of magnetic moments in many odd-mass nuclei have shown that the quantity κ can be chosen in the form

$$\kappa = 1.5 \frac{N-Z}{A} [\text{MeV}] . \quad (27)$$

The strong isospin-dependence of κ leads to the conclusion that the isovector part of the residual force gives the main contribution to the spin-polarization effects (see the discussion in ref. /9/). Eq. (27) is used in all the calculations discussed below.

The intrinsic quadrupole moment Q_0 is considered as a free parameter because the large dispersion of experimental values obtained by means of different methods (see, e.g., review articles /10/) does not allow in many cases, to do the unique choice. Our choice of the Q_0 value usually proceeds from the fit of calculations to experimental intensity ratio λ_I . It is necessary to emphasize that when the nonadiabatic corrections in eq. (22) become signi-

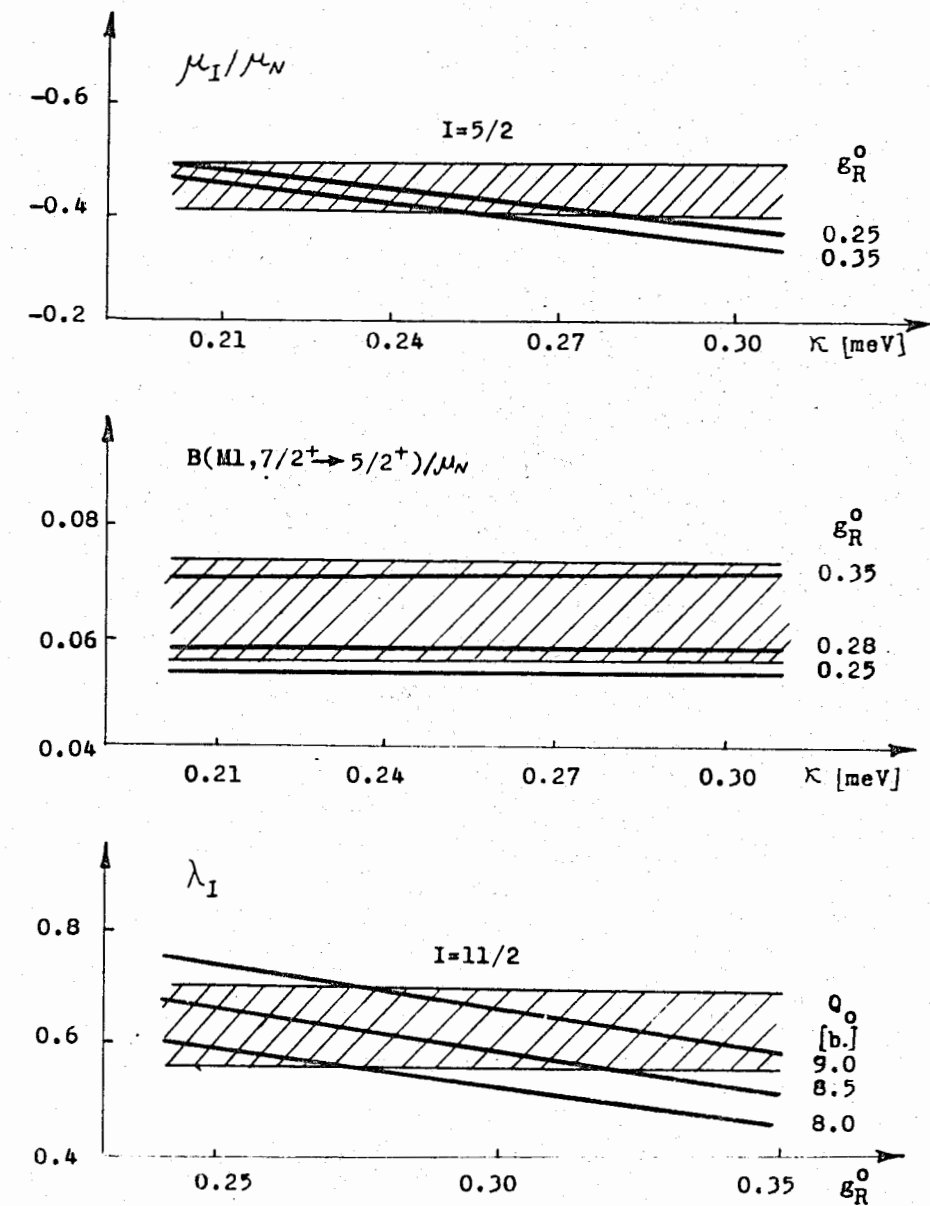


Fig. 3. The dependence of μ_I , $B(\text{MI})$ and λ_I on the model parameters is shown for a few states of the ground band of ^{161}Dy . Experimental data (shaded areas) are from refs. /19, 21, 23/.

ficant, the value of Q_0 used in our calculations of λ_1 may be noticeably larger than that derived from the experimental $B(E2)$ value in adiabatic limit /10/. The difference between our parameter Q_0 and the corresponding value in neighbouring even-even nuclei can occur because the coupling of quasiparticles to the quadrupole excitations of the core is disregarded. Collective admixtures due to this coupling are usually small in the low-energy states (see, e.g., ref. /11/), so that one can hope that they do not affect noticeably the intraband E2-transition probabilities.

The dependence of the $B(MI)$ and λ_1 values on the parameters κ , g_R^0 and Q_0 is shown in Fig. 3 for some states of the ground rotational band in ^{161}Dy .

Numerical results for a number of rare-earth nuclei are listed in tables I-4 ^{x/}, where are given the mixing amplitudes C_k , rotational energies, decoupling parameter $\alpha(I)$ values, magnetic moments μ_I , effective g_R^{eff} factors, transition probabilities and intensity ratios. On the whole, the calculated quantities agree with the presently known experimental data. Below we discuss some results of these calculations.

I. The consideration of the centrifugal and spin polarization as well as the Coriolis force allows one to explain the empirical magnetic moments in odd-mass nuclei, using the g_R^0 factors close to those in the neighbouring even-even nuclei. The calculated g_R^{eff} factors agree well, as a rule, with the corresponding experimental values estimated from the magnetic moments and $B(MI)$ values in adiabatic limit (see, e.g., refs. /5,6/). But, as a rule, the calculated g_R^{eff} are not constant in the rotational band. This evokes the strong difference between the calculated μ_I and those estimated in adiabatic approximation using the empirical g_K and g_R parameters (see table I). Note that for high-spin states ($I \gg 1$) the quantity $\mu_I \sim g_R^{\text{eff}} I$ and g_R^{eff} estimated from eq. (17) becomes very close to that calculated from eq. (15). The comparative behaviour of g_R^{eff} in odd-N and odd-Z nuclei is shown in Fig. 4 for the ground state rotational bands in ^{167}Er and ^{165}Ho .

^{x/} The calculated mixing amplitudes and energies in ^{161}Dy , ^{177}Hf and ^{179}Hf are slightly different from those of ref. /2/ which is connected with the change of parameters used in calculations.

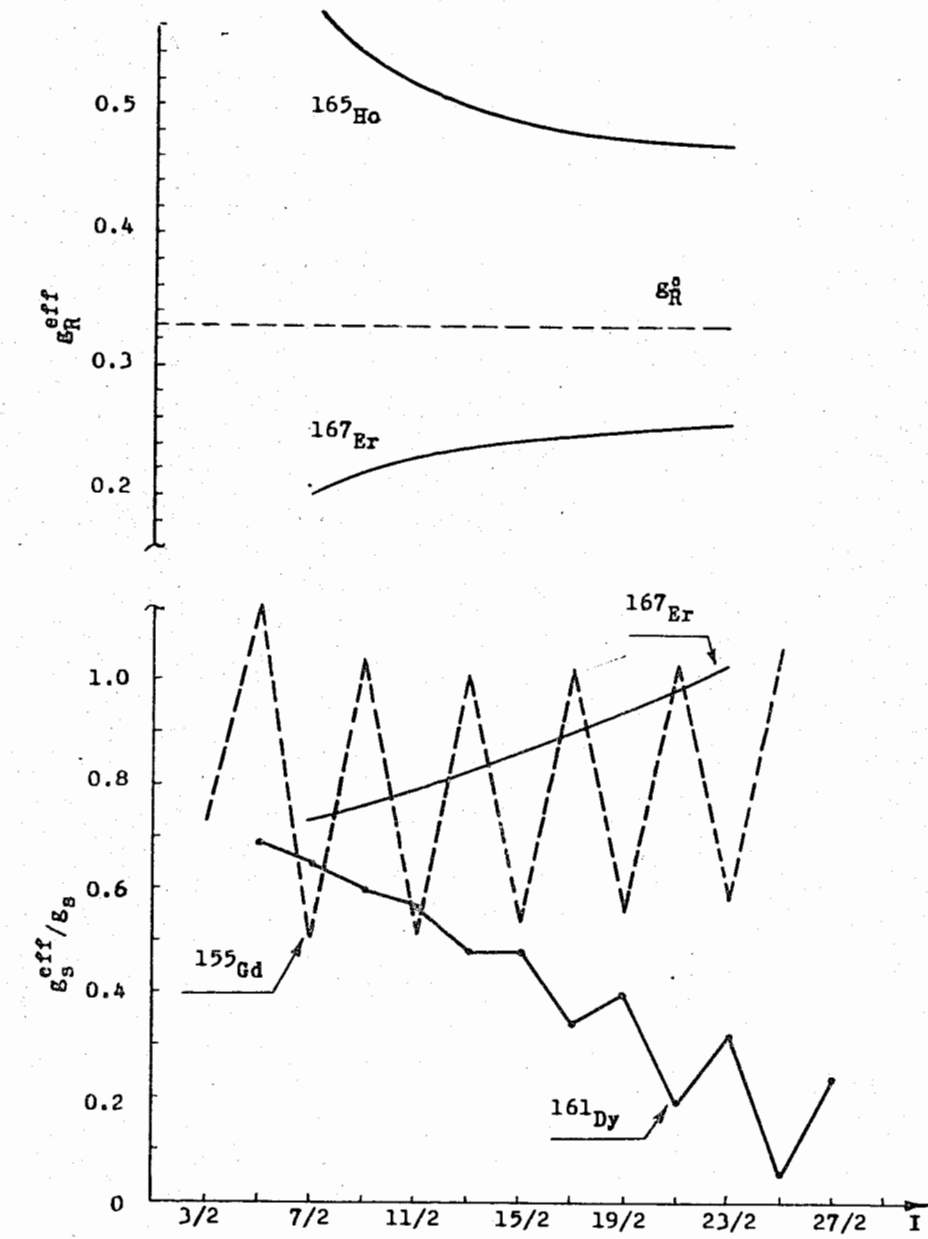


Fig. 4. Effective g_R^{eff} factors (above) and g_s^{eff} factors (below) versus spin value for the ground bands of some nuclei (positive parity quasirotational band in ^{155}Gd).

2. When the Coriolis coupling is weak the renormalization of the g_s -factor is determined by R_σ ($K > 1/2$). The Coriolis coupling does not allow one to separate the longitudinal and transverse polarization effects. The behaviour of g_s^{eff} (eq. (18)) in the rotational band now depends on the relative sign of both effects (see Fig. 4). The contributions from the longitudinal and transverse terms may be of the same sign (as in ^{167}Er), of opposite sign (^{161}Dy), or their signs may change from state to state (g_s^{eff} fluctuates in ^{155}Gd). Reliable information about g_s^{eff} can be obtained through measurements of the magnetic moments of the low-spin rotational states.

3. A very complicated spectrum of positive parity states is found in ^{155}Gd (see, e.g., refs. /12, 13/). One can obtain a satisfactory theoretical description of this spectrum taking into account the Coriolis coupling of single-particle states originating from the spherical subshell $i_{13/2}$. But in the usual method of least-square fitting one uses a large number of parameters (quasi-particle energies, rotational parameters, N-mixing parameters, parametrization of the spin-polarization, etc.) /12-14/.

In our calculations the theoretical quasiparticle spectrum has been used (calculations are performed with $\beta_{20} = 0.32, \beta_{40} = 0$ and $\Delta = 0.6$ MeV). The other parameters and the numerical results are listed in table 2. The deformation parameter is chosen from the best fit of the calculations to the experimental magnetic moments of the lowest-energy $5/2^+$ and $3/2^+$ states and the probabilities for γ -transition between them (see Fig. 5). The calculated magnetic moments agree well with those reported by Blumberg et al. /15/, but are in disagreement with those of refs. /16/. The theory reproduces surprisingly well the whole spectrum of the $5/2^+$ states and the sequence of states belonging to the quasirotational band (marked with asterisk in table 2). The nonadiabatic effects are especially strong in low-energy states which are characterized by the very unusual effective parameters x ($g_R^{\text{eff}} \leq 0$,

g_s^{eff} strongly fluctuates). The nonadiabatic effects are pronounced in the ratio of the spectroscopic quadrupole moments Q_1 for the states of the quasirotational band to the corresponding quantity for the ground state $Q_{\text{g.r.t.}}(3/2^+[521])$, as is shown in Fig. 6.

^x/ The quantities g_R^{eff} and g_s^{eff} displayed in table 2 and Fig. 4 are calculated assuming that the quasirotational band is built on the $3/2^+[651]$ state.

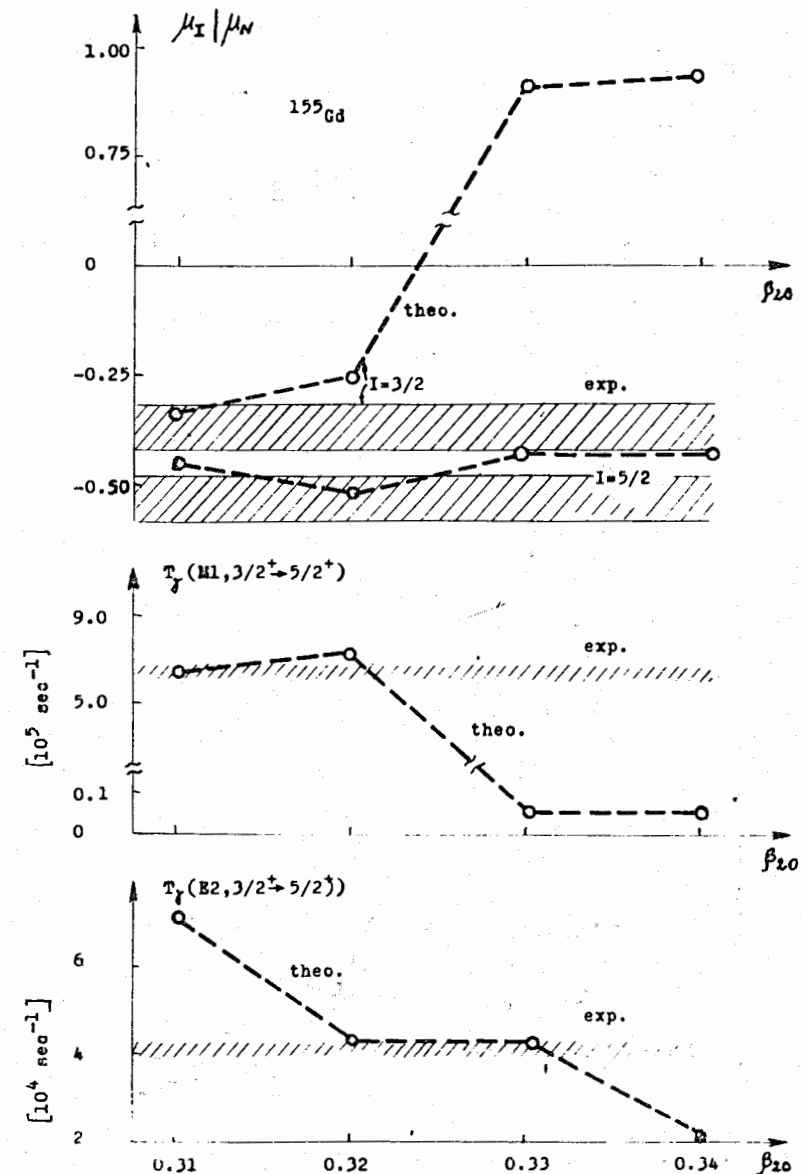


Fig. 5. Magnetic moments of the lowest-energy $5/2^+$ and $3/2^+$ states in ^{155}Gd and the probabilities of MI and E2 transitions between them versus the deformation parameter. Experimental data (shaded areas) are from refs. /15, 27/.

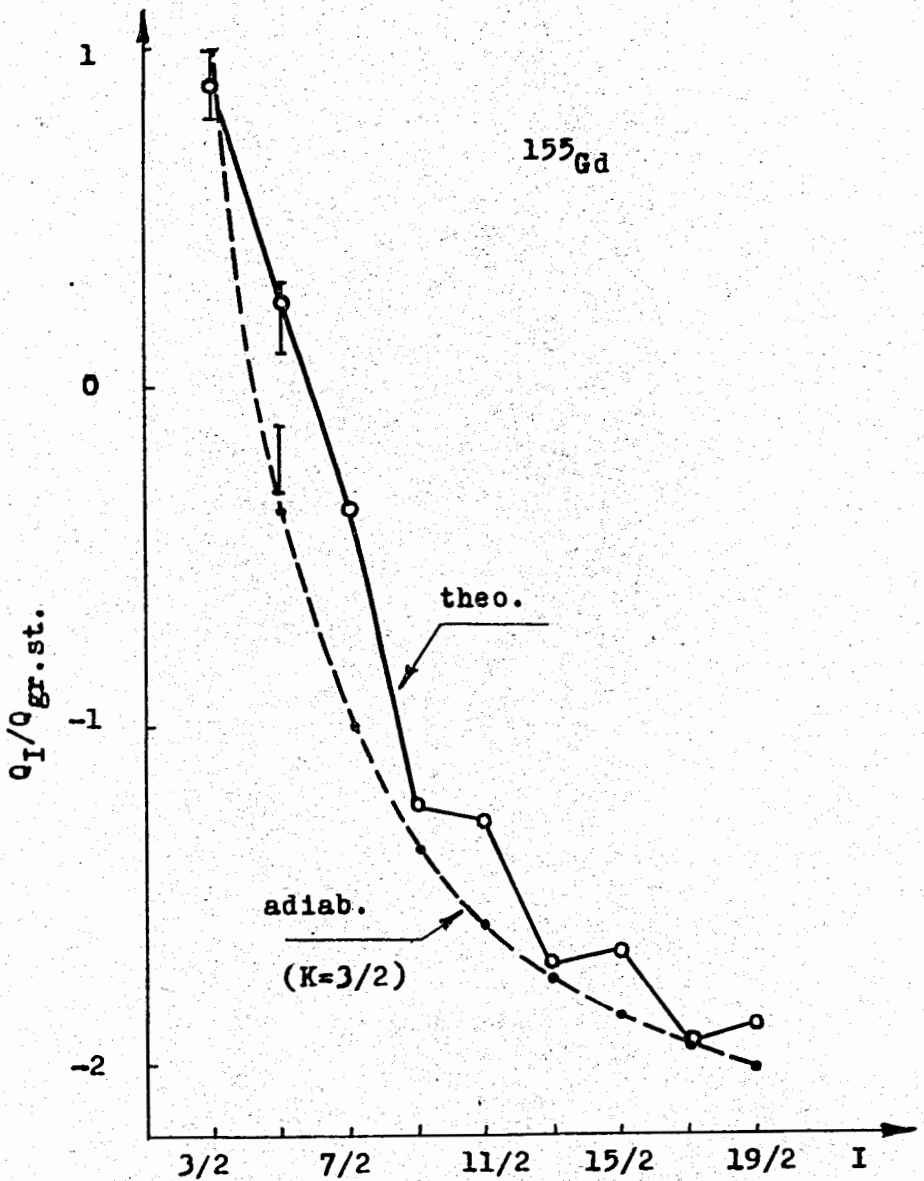


Fig. 6. The ratio of the spectroscopic quadrupole moments Q_I for the states of the quasirotational band in ^{155}Gd to the corresponding quantity for the ground state. Experimental data are taken from refs./15/.

The predicted ratio is in good agreement with the experimental data of ref. /15/.

4. Two rotational bands are studied in detail in ^{177}Hf , the ground state band (negative parity) and the band built on the excited $9/2^+[624]$ state (see, e.g., refs. /17-19/). We have made an attempt to describe both bands using one set of collective parameters Δ , g_R^0 and Q_0 (rotational parameter $1/2 J$ is obtained for each band from the least-square fit to experimental energies). The results of calculations are displayed in table 3. In the ground state band the admixtures are small. The dynamic effects in this band are noticeable starting from the spin value $I = 17/2$ (the stretching and CAP effects in the core). Analogous effects in the positive parity band occur at much higher spin values.

The $B(\text{MI})$ values in the ground band are extremely sensitive to the choice of g_R^0 . The empirical values of $B(\text{MI}, 11/2^- \rightarrow 9/2^-) = -(2.2 \pm 1.1) 10^{-3} \mu_N^2$ and δ^2 , given in refs. /19,20/ can be well reproduced with $g_R^0 = 0.23$. The quantity λ_I in this band does not practically depend on g_R^0 . The calculated values of λ_I agree well with the data of refs. /17,18/. The properties of the $9/2^+[624]$ rotational band in both the ^{177}Hf and ^{179}Hf (table 4) nuclei are much less sensitive to g_R^0 . A reasonable agreement with experimental data may be obtained with $0.23 \leq g_R \leq 0.30$. To fix this parameter one needs to measure the magnetic moments of a few rotational states in the band. The same is valid for the ground band in ^{167}Er (table 4).

Conclusion

The present paper completes a series devoted to the study of rotational motion in odd-mass nuclei in the framework of nonadiabatic rotational model. The model takes into account the Coriolis coupling of the odd particle to the core as well as a number of polarization effects generated by the coupling of the odd nucleon to the intrinsic 1^+ excitations in the core. This approach allows one to obtain a satisfactory description of all the properties of a single rotational band using the minimal number of collective parameters of the core. The effective parameters for the odd-mass nucleus are calculated in the model.

Below we discuss some approximations used in the model.

i) Static approximation for the pairing correlations in the core ($\Delta = \text{const.}$). This restriction becomes of importance for the high spin states. The solution of the dynamical equation for the energy gap in odd-mass nuclei has shown that the Coriolis coupl-

ing of the odd particle to the core stabilizes the energy gap and the moment of inertia thus relaxing the CAP effects in the core /28/.

ii) The quadrupole vibrations of the core are not included in the model. For this reason it is difficult at present to describe a few rotational bands of the same parity using one set of parameters. The inclusion of the quadrupole and octupole vibrations in the model does not bring any difficulties of principle.

iii) The intrinsic Hamiltonian is not rotational invariant. Hence, among I^+ states there is one spurious state belonging to the collective rotational branch (see, e.g., refs. /29/). The spurious state was not separated when considering the polarization effects. But due to the smallness of the three-quasiparticle admixtures, the error associated with the spurious state is believed to be negligible.

iv) We have not studied the effects connected with the five-(and more) quasiparticle admixtures, which arise from anharmonicities of vibrations of the core.

In conclusion the authors wish to express their gratitude to the members of the Nuclear Theory Department for the discussion of this work. Thanks are due to S.I. Fedotov, S.I. Gabrakov and H. Schulz for supplying the computer codes utilized in calculations of the Saxon-Woods single-particles energies and matrix elements.

References

1. N.I. Pyatov, M.I. Chernej, M.I. Baznat. JINR, E4-5468, Dubna, 1970.
2. M.I. Chernej, M.I. Baznat, N.I. Pyatov. JINR, E4-5550, Dubna, 1970.
3. A.A. Kuliev, N.I. Pyatov. Yadernaya Fizika, 9, 313, 955 (1969).
4. S.G. Nilsson. Kgl.Dan.Vid.Selsk. Mat.Fys.Medd., 29, No 16 (1955).
5. L. Grodzins. Ann.Rev.Nucl.Sci., 18, 291 (1968).
6. Ju.T. Grin, I.M. Pavlichenkov. JETP, 41, 954 (1961).
A. Hrynkiewicz, S. Ogaza. Structura slojnyh yader (Atomizdat, Moskva, 1966), p. 272.
7. O. Prior, F. Boehm, S.G. Nilsson. Nucl.Phys., A110, 257 (1968).
7. F.A. Gareev, S.P. Ivanova, B.N. Kalinkin. Izv.Akad.Nauk SSSR, ser.fiz., 32, 1960 (1968).

8. V.G. Soloviev, S.I. Fedotov. JINR, E4-6055, Dubna, 1971.
9. A. Bohr, B.R. Mottelson. Nuclear Structure. (Benjamin, N.Y., 1969), v.1, ch. 3.
10. B.S. Djalepov. Structura slojnyh yader (Atomizdat, Moskva, 1966), p. 189.
G.H. Fuller, V.W. Cohen. Nucl.Data, A5, 433 (1969).
11. K.E.G. Löbner, M. Vetter, V. Höning. Nucl.Data, A7, 495 (1970).
11. L.A. Malov, V.G. Soloviev, S.I. Fedotov. Izv.Akad.Nauk SSSR, ser.fiz., 35, 747 (1971).
12. J. Borggreen, G. Løvhøiden, J.C. Waddington. Nucl.Phys., A131, 241 (1969).
13. G. Løvhøiden, J.C. Waddington et al. Nucl.Phys., A148, 657 (1970).
14. M.E. Bunker, C.W. Reich. Phys.Lett., 25B, 396 (1967).
15. H. Blumberg, B. Persson, M. Bent. Phys.Rev., 170, 1076 (1968).
16. A. Hrynkiewicz, S. Ogaza et al. Nucl.Phys., 80, 608 (1966).
R.A. Begjanov et al. Izv.Akad.Nauk SSSR, ser.fiz., 35, 135 (1971).
17. P. Alexander, F. Boehm, E. Kankeleit. Phys.Rev., 133, B284 (1964).
18. A.J. Haverfield, F.M. Bernthal, J.M. Hollander. Nucl.Phys., A94, 337 (1967).
19. H. Hübel, C. Günter et al. Nucl.Phys., A127, 609 (1969).
20. E.M. Bernstein, J. deBoer. Nucl.Phys., 18, 40 (1960).
21. A. Johnson, S.A. Hjørth, H. Ryde. Annual Report 1969 AF1, Stockholm, p. 22.
22. D. Ashery, N. Bahcall et al. Nucl.Phys., A101, 51 (1967).
23. G.B. Hagemann, A. Tveter. Phys.Lett., 26B, 136 (1968).
24. W. Michaelis, F. Weller et al. Nucl.Phys., A143, 225 (1970).
25. F. Boehm, G. Goldring et al. Phys.Lett., 22, 627 (1966).
26. H. Hübel, R.A. Naumann. Phys.Rev., C1, 1845 (1970).
27. A. Krusche, D. Bloess, F. Münnich. Z.Physik, 192, 490 (1966).
28. M.I. Chernej, N.I. Pyatov, V.Ju. Keloglu. JINR, D6-5783, Dubna, 1971, p. 4.
29. B.L. Birbrair. Nucl.Phys., A108, 449 (1968); V.M. Mikhailov. Izv.Acad.Nauk SSSR, ser.fiz., 34, 840 (1970).

Received by Publishing Department
on February 4, 1972.

Table 1

Characteristics of the ground state rotational band in ^{161}Dy . Calculations are performed with $1/2\gamma = 12.1$ kev, $g_R^0 = 0.28$ and $Q_0 = 8.5$ b.

I^π	Mixing amplitudes C_K^I						$\mu_{I,1}^a$ [kev]	$\mu_{I,2}^b$ [kev]	$B(M1)$ $\delta_I^{(b)}$ $\times 10^{-2}$	λ_I^d	
	[400] ^t	[660] ^t	[651] ^t	[642] ^t	[633] ^t	[624] ^t					
5/2	0.0II	0.03I	0.18I	0.983	-	-	I.12	0	-0.4I	-0.46	0.II
7/2	0.0I4	0.040	0.255	0.950	0.17I	-	-2.45	42	44	-0.07	-0.018
9/2	0.034	0.097	0.32I	0.912	0.230	0.015	3.56	97	I00	0.23	0.03
11/2	0.026	0.07I	0.349	0.89I	0.273	0.027	-3.94	I79	I84	0.55	0.2I
13/2	0.059	0.170	0.406	0.845	0.289	0.035	4.89	266	267	0.80	0.37
15/2	0.035	0.096	0.406	0.846	0.323	0.046	-4.68	398	407	I.I4	0.52
17/2	0.084	0.24I	0.464	0.786	0.310	0.050	5.74	513	508	I.37	0.67
19/2	0.042	0.115	0.442	0.812	0.35I	0.063	-5.10	707	719	I.72	0.80
21/2	0.106	0.303	0.502	0.733	0.314	0.060	6.32	845	826	I.92	0.93
23/2	0.048	0.129	0.466	0.785	0.370	0.078	-5.37	II07	III9	2.30	I.06
25/2	0.125	0.355	0.527	0.688	0.309	0.068	6.74	I264	I222	2.48	I.I9
27/2	0.052	0.140	0.482	0.764	0.383	0.092	-5.54	I60I	I602	2.87	I.3I
29/2	0.140	0.397	0.544	0.65I	0.302	0.073	7.0I	I774	I693	3.04	I.43
31/2	0.056	0.149	0.495	0.747	0.393	0.104	-5.67	II90	II62	3.44	I.55
33/2	0.153	0.43I	0.555	0.619	0.293	0.078	7.22	2375	2235	3.60	I.67

a) taken from ref/21/; b) calculated with $g_K = -0.30$ and $g_R^{\text{eff}} = 0.11$ (ref/23/). Experimental value of $\mu_{5/2} = -(0.46 \pm 0.05)$ (ref/10/). c) experimental values of δ_I equal to 0.047, 0.066 and 0.048 (± 0.007) for the spin values 9/2, 11/2 and 13/2 respectively (ref/23/). d) experimental values of $\lambda_{11/2} = 0.63 \pm 0.07$ and $\lambda_{13/2} = 1.6 \pm 0.7$ are given in ref/23/.

Table 2

Positive parity states in ^{155}Gd . Calculations are performed with $1/2\gamma = 13.2$ kev, $g_R^0 = 0.33$ and $Q_0 = 8.5$ b.

I^π	Mixing amplitudes C_K^I						$\mu_{I,1}^a$ theo. [kev]	$\mu_{I,2}^b$ exp./13/a(I) [kev]	$B(M1)$ δ_I^2 $\times 100$ [$e^2 b^2$]	$B(E2)$ [$e^2 b^2$]	$\lambda_I X_{13}^I$ theo. exp.	
	[660] ^t	[400] ^t	[651] ^t	[402] ^t	[642] ^t	[633] ^t						
* 3/2 ⁺	0.2II	0.067	0.974	-0.042	-	-	I77	I05.3	-I.42	-0.24	-0.04	0.65
3/2 ⁺	-0.05I	0.035	0.05I	0.997	-	-	266	268.6	-0.08	0.96	0.32	
3/2 ⁺	-0.575	0.812	0.066	-0.06I	-	-	668	427.I	-0.08	0.42	0.29	
* 5/2 ⁺	0.370	0.118	0.703	-0.082	0.590	-	86.6	86.6	5.24	-0.52	-0.13	
5/2 ⁺	0.490	0.142	0.367	-0.030	-0.777	-	268	266.5	I.16	-0.08	0.38	
5/2 ⁺	-0.080	0.048	0.155	0.984	-0.007	-	33I	325.9	0.10	I.15	0.32	
5/2 ⁺	0.759	0.115	-0.584	0.149	0.217	-	513	488.6	-I.93	0.88	0.30	
* 7/2 ⁺	0.190	0.064	0.682	-0.082	0.693	0.089	I25	II8.0	-4.34	-0.06	0.10	0.9
* 9/2 ⁺	0.485	0.160	0.676	-0.092	0.515	0.089	99	I07.6	6.84	0.12	0.07	I.3
* II/2 ⁺	0.2I3	0.074	0.675	-0.089	0.680	0.154	237	230.3	-5.03	0.64	0.18	2.5
* I3/2 ⁺	0.543	0.184	0.653	-0.094	0.472	0.II3	2I2	2I4.3	7.37	0.78	0.14	
* I5/2 ⁺	0.223	0.080	0.665	-0.09I	0.674	0.197	455	453.6	-5.36	I.32	0.22	3.1
* I7/2 ⁺	0.576	0.198	0.636	-0.094	0.447	0.I27	430	423.7	7.60	I.44	0.19	
* I9/2 ⁺	0.227	0.083	0.655	-0.092	0.670	0.230	777	786.6	-5.56	I.99	0.24	3.4
* I2I/2 ⁺	0.596	0.207	0.624	-0.094	0.430	0.I37	75I	736.7	7.72	2.I0	0.2I	
* I23/2 ⁺	0.229	0.084	0.646	-0.092	0.668	0.258	I203	I220.I	-5.70	2.66	0.25	3.6
* I25/2 ⁺	0.6I0	0.2I3	0.6I4	-0.094	0.4I8	0.I44	II76	II44.4	7.80	2.76	0.13	0.69

Calculated are $B(M1)$, $B(E2)$ and δ_I^2 values for the energy-allowed transitions from a given level to the levels of the quasirotational band marked with asterisk (upper line corresponds to $I \rightarrow I-1$ transition, the lower one to $I \rightarrow I+1$ transition).

Table 3

Rotational bands in ^{177}Hf . Calculations are performed with $g_R^0=0.23$, $Q_0=7.6 \text{ b}$, $1/2\gamma=13.4 \text{ kev}$ (negative parity band) and 14.6 kev (positive parity band). Only the largest mixing amplitudes are given.

I	Mixing amplitudes C_K^I				$\delta(I)$ theo. [kev]	$\delta(I)/19/\mu_I$ exp. [kev]	μ_I theo. [μ_N]	(I → I-1)		$\delta_I^2 \times 10$	λ_I theo.	λ_I exp./18/
	[532] †	[523] †	[514] †	[505] †				ϵ_R^{eff} x100 [μ_N^2]	B(M1) [μ_N^2]	B(E2) [$e^2 b^2$]		
7/2 $^-$	0.003	0.056	0.998	-	0	0	0.87	0.20	-	-	-	-
9/2 $^-$	0.006	0.085	0.996	0.030	III	III, 0	1.06	0.21	0.10	1.94	18.2	-
II/2 $^+$	0.009	0.110	0.993	0.050	247	249,7	1.26	0.21	0.15	1.96	17.6	4.1
I3/2 $^+$	0.013	0.133	0.989	0.064	408	409.4	1.47	0.21	0.18	1.68	17.1	9.6
I5/2 $^+$	0.017	0.155	0.985	0.076	594	591.3	1.68	0.21	0.19	1.39	16.6	16.5
I7/2 $^+$	0.022	0.175	0.980	0.087	804	794.4	1.89	0.21	0.21	1.15	16.1	29.4
I9/2 $^+$	0.027	0.195	0.975	0.097	I040	I017.7	2.10	0.21	0.21	0.95	15.6	34.7
21/2 $^+$	0.033	0.215	0.970	0.107	I300	I260.3	2.31	0.21	0.22	0.81	15.1	45.8

I	Mixing amplitudes C_K^I				$\delta(I)$ theo. [kev]	$\delta(I)/19/\mu_I$ exp. [kev]	μ_I theo. [μ_N]	ϵ_R^{eff} x10 [μ_N^2]	(I → I-1)		$\delta_I^2 \times 10$	λ_I theo.	λ_I exp./18/
	[642] †	[633] †	[624] †	[615] †					B(M1) [μ_N^2]	B(E2) [$e^2 b^2$]			
9/2 $^+$	0.031	0.194	0.980	-	0	0	-0.80	0.14	-	-	-	-	-
II/2 $^+$	0.055	0.271	0.951	0.139	I04	I05,3	-0.43	0.15	0.11	1.77	1.28	-	-
I3/2 $^+$	0.079	0.325	0.923	0.188	232	233.8	-0.09	0.16	0.18	1.98	1.31	0.37	0.35 (4)
I5/2 $^+$	0.103	0.368	0.897	0.221	384	387.1	0.21	0.16	0.22	1.82	1.35	0.87	0.81 (8)
I7/2 $^+$	0.126	0.402	0.872	0.244	563	561.5	0.50	0.17	0.26	1.58	1.31	1.54	1.42 (14)
I9/2 $^+$	0.148	0.430	0.850	0.261	767	765.6	0.78	0.17	0.28	1.35	1.40	2.20	1.95 (20)
21/2 $^+$	0.170	0.454	0.828	0.274	998	980.0	1.05	0.17	0.30	1.15	1.24	3.42	3.35 (42)

Experimental data: $\mu_{7/2}=-0.780(21)$ and $\mu_{9/2}=-0.725(85)/18/$, $\mu_{9/2}=1.04(6)$ and $\mu_{11/2}=1.52(44)/5/$.

Table 4
Ground state rotational bands in ^{167}Er and ^{179}Hf .

I	Mixing amplitudes C_K^I				$\delta(I)$ theo. [kev]	$\delta(I)$ exp. [kev]	μ_I theo. [μ_N]	ϵ_R^{eff} x10 [μ_N^2]	(I → I-1)		$\delta_I^2 \times 10$	λ_I theo.	λ_I exp.
	[651] †	[642] †	[633] †	[624] †					B(M1) [μ_N^2]	B(E2) [$e^2 b^2$]			
^{167}Er ($1/2\gamma=13.1 \text{ kev}$, $g_R^0=0.33$, $Q_0=8.3 \text{ b}$)													
7/2 $^+$	0.018	0.151	0.988	-	-	0	0	-0.59	0.20	-	-	-	-
9/2 $^+$	0.034	0.217	0.968	0.123	-	77	79.3	-0.14	0.22	0.12	2.27	0.86	-
11/2 $^+$	0.051	0.269	0.946	0.173	0.009	175	177.6	0.25	0.23	0.18	2.28	0.84	0.33 0.34(2)
13/2 $^+$	0.070	0.311	0.924	0.208	0.016	293	293.7	0.62	0.23	0.23	1.94	0.81	0.77 0.80(5)
15/2 $^+$	0.086	0.345	0.904	0.235	0.022	433	432.4	0.98	0.24	0.26	1.60	0.84	1.27 1.32(14)
17/2 $^+$	0.107	0.376	0.883	0.255	0.028	595 (592.0)	1.32	0.25	0.28	1.32	0.84	2.01	-
19/2 $^+$	0.120	0.400	0.865	0.272	0.034	780 (772.0)	1.67	0.25	0.29	1.09	0.84	2.87	-
^{179}Hf ($1/2\gamma=14.5 \text{ kev}$, $g_R^0=0.26$, $Q_0=7.8 \text{ b}$)													
9/2 $^+$	0.002	0.018	0.143	0.989	-	0	0	-0.66	0.19	-	-	-	-
11/2 $^+$	0.005	0.034	0.206	0.972	0.112	121	122.7	-0.22	0.20	0.12	1.85	1.52	-
13/2 $^+$	0.008	0.050	0.255	0.953	0.156	267	268.9	0.17	0.20	0.21	2.08	1.51	0.44 0.416(35)
15/2 $^+$	0.013	0.067	0.295	0.934	0.188	437	438.9	0.52	0.21	0.26	1.92	1.50	0.99 1.045(45)
17/2 $^+$	0.018	0.085	0.330	0.915	0.213	632	631.5	0.85	0.21	0.30	1.68	1.48	1.67 1.34 (18)
19/2 $^+$	0.024	0.103	0.360	0.897	0.232	852	848.5	1.14	0.21	0.33	1.44	1.47	2.43 2.37 (18)
21/2 $^+$	0.031	0.121	0.386	0.879	0.247	1099	1085.2	1.47	0.22	0.35	1.24	1.44	3.38 3.61 (20)

Experimental data: δ_I and λ_I for ^{167}Er from refs/24,25/; $\mu_{7/2}=-0.564(7)/10/$; $\delta(I)$, λ_I and $\mu_{9/2}=-0.611(17)$ for ^{179}Hf from ref./26/.